JOURNAL OF MATERIALS SCIENCE 21 (1986) 1525–1532

The effect of strain rate, temperature and texture on anisotropic deformation in Ti–6Al–4V

D. S. McDARMAID, P. G. PARTRIDGE
Materials and Structures Department, Royal Aircraft Establishment, Farnborough, Hampshire, UK

The effect of temperature and strain rate on the transition between grain-boundary sliding and slip-controlled deformation in Ti–6Al–4V at elevated temperatures has been determined by measuring the strain anisotropy. The anisotropy below the transition was dependent on texture, but above the transition was dependent on contiguous α-phase.

1. Introduction

In order to improve the superplastic behaviour of alloys, attempts have been made to relate superplastic flow to microstructure, texture and processing parameters [1, 2]. Deformation models for superplasticity refer to single-phase systems [3] and depend upon a knowledge of the deformation modes active under superplastic conditions [2–4]. In tests on commercial alloys at elevated temperatures, it is often difficult to determine the dominant deformation mode and to relate it to the microstructure existing only at the deformation temperature. This task is particularly difficult for α-β titanium alloy tested at about 900° C in an inert atmosphere, since annealing and phase transformation occur during cooling at room temperature.

Recent studies [5, 6], have shown that in two-phase alloys the phase distribution can affect the uniformity of superplastic flow. For example in textured Ti–6Al–4V alloy bar the stress and strain anisotropy were different during superplastic and non-superplastic deformation. The strain anisotropy is illustrated in Fig. 1 which shows the initially round cross-sections of test pieces oriented parallel to the short transverse (ST) direction became elliptical after tests at both 20 and 928° C. However, the long axis of the ellipse was parallel to the transverse (T) direction (the 0002 pole axis) at 20° C (Fig. 1a) when dislocation glide was the dominant deformation mode, and normal to this direction after superplastic deformation (Fig. 1b) when grain-boundary sliding was the dominant deformation mode. The anistropy under superplastic conditions was explained in terms of a two-phase deformation model [7], which depended upon the greater resistance to grain-boundary sliding in the α/α grain boundaries than in α/β or β/β grain boundaries in the banded microstructure.

This relationship between the sense of the strain anisotropy and the controlling deformation mode has been used to monitor the change in deformation mode in Ti–6Al–4V when the test conditions (i.e. strain rate and temperature) were varied within and outside the superplastic range. The results obtained in these tests are described in this paper and used to clarify the role of crystallographic texture and to indicate the processing limits in superplastic forming of thin Ti–6Al–4V sheet.

2. Experimental techniques

The Ti–6Al–4V alloy tested had a composition (wt %) of 6.3 Al, 4.4 V, 0.18 Fe, $< 0.006\,H_2$, $< 0.01\,N_2$, 0.150_2, balance Ti. It was supplied in the form of hot-rolled rectangular bar with a cross-section 160 mm × 50 mm. Prior to machining the bar was mill annealed 4 h at 700° C and air cooled. The bar had a strong α-phase basal texture with the 0002 poles parallel to the long transverse direction (T) as shown in Fig. 2; this texture was not significantly affected by heating to the superplastic deformation temperatures used in this paper. The microstructure at elevated temperatures, contained regions of aligned and contiguous fine-grained α-phase (Band A) in a randomly distributed fine grained α and β microstructure (Band B) as shown in Fig. 3.

Round bar test pieces with gauge diameters of either 4 or 13 mm and a gauge length of 22 mm were machined from the bar with the text piece axis oriented parallel to the short transverse (ST) direction. The longitudinal (L, rolling) direction was marked on the end cross-section of each test piece. Room and elevated temperature uniaxial tensile tests were carried out to a maximum of ~260% elongation in deoxygenated argon atmosphere within a silica tube with the temperature maintained at $T \pm 2°$ C in a triple-zone vertical furnace. The test piece was held 0.5 h at temperature prior to testing at constant cross-head speeds with the initial strain rates in the range 4.2×10^{-4} to $1.05 \times 10^{-1}\,sec^{-1}$ over the temperature range 20 to 970° C. The volume fraction of the α phase present at each temperature was determined by metallographic analysis of sample material water quenched after a 0.5 h hold at temperature in an argon atmosphere.

The anisotropy observed in the gauge length was monitored using the ratio dP/dN, where dP and dN are the diameters of the gauge length parallel and normal, respectively, to the 0002 poles of the α-phase. These diameters were measured with a travelling microscope.

0022–2461/86 $03.00 + .12

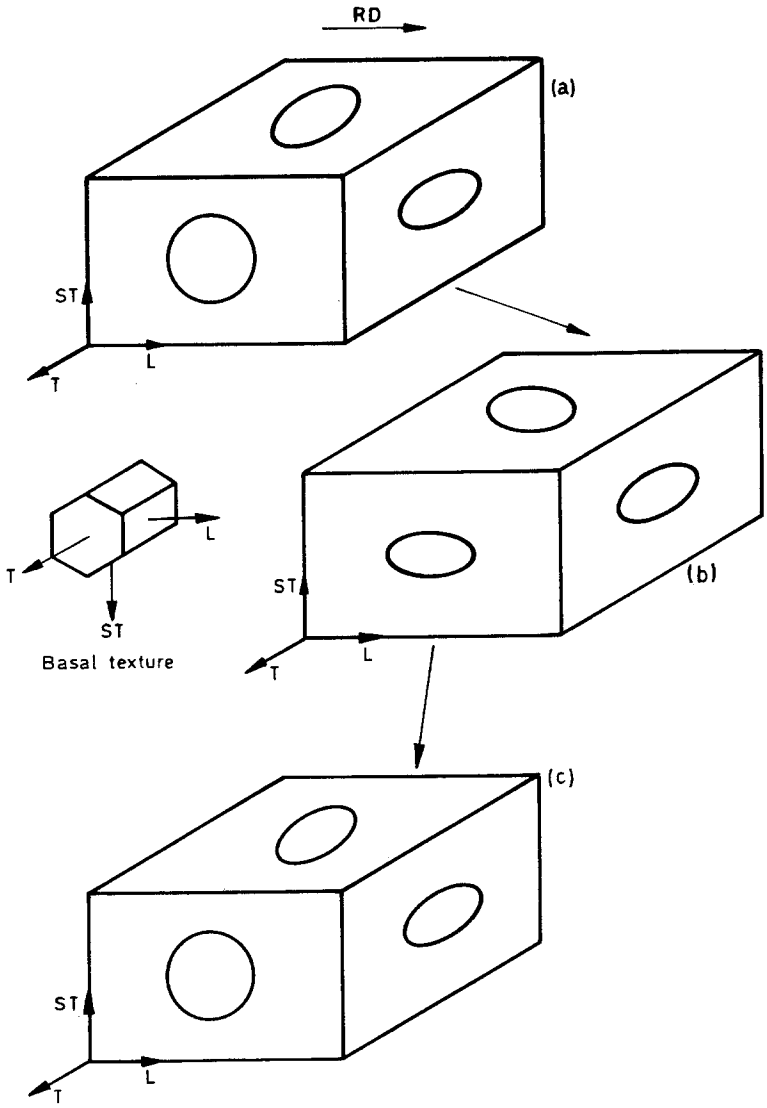

Figure 1 Schematic diagram of Ti–6Al–4V test piece cross-section after uniaxial strain. (a) After strain at room temperature, Mill annealed material. (b) After superplastic strain at elevated temperature. (c) After strain at room temperature, following superplastic strains up to 344%.

3. Results

3.1. Effect of strain rate

The flow stress (σ) against initial strain rate ($\dot{\varepsilon}_I$) curves obtained at various test temperatures are plotted in Fig. 4. Superplastic deformation was obtained at 900 to 928° C for strain rates less than $10^{-2}\,\text{sec}^{-2}$; these conditions correspond to high m values where

$$m = \frac{\delta \ln \sigma}{\delta \ln \dot{\varepsilon}_I}$$

The dP/dN ratios obtained for 13 and 4 mm diameter test pieces deformed at 928 and 900° C respectively

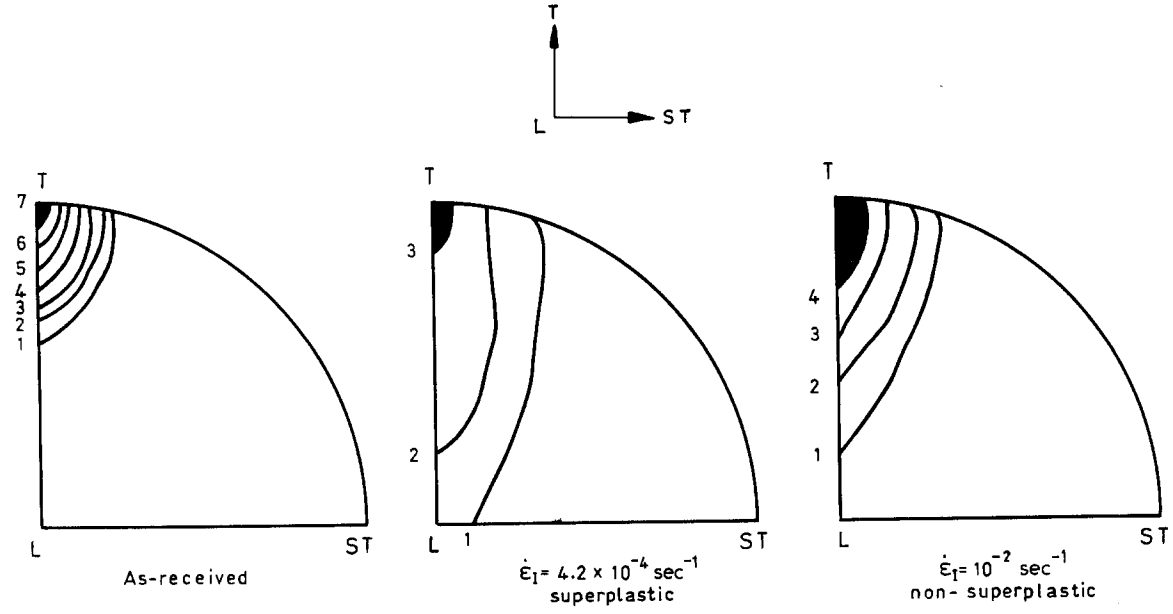

Figure 2 Effect of 300% longitudinal strain at 928° C on the α-phase (0 0 0 2) pole figures.

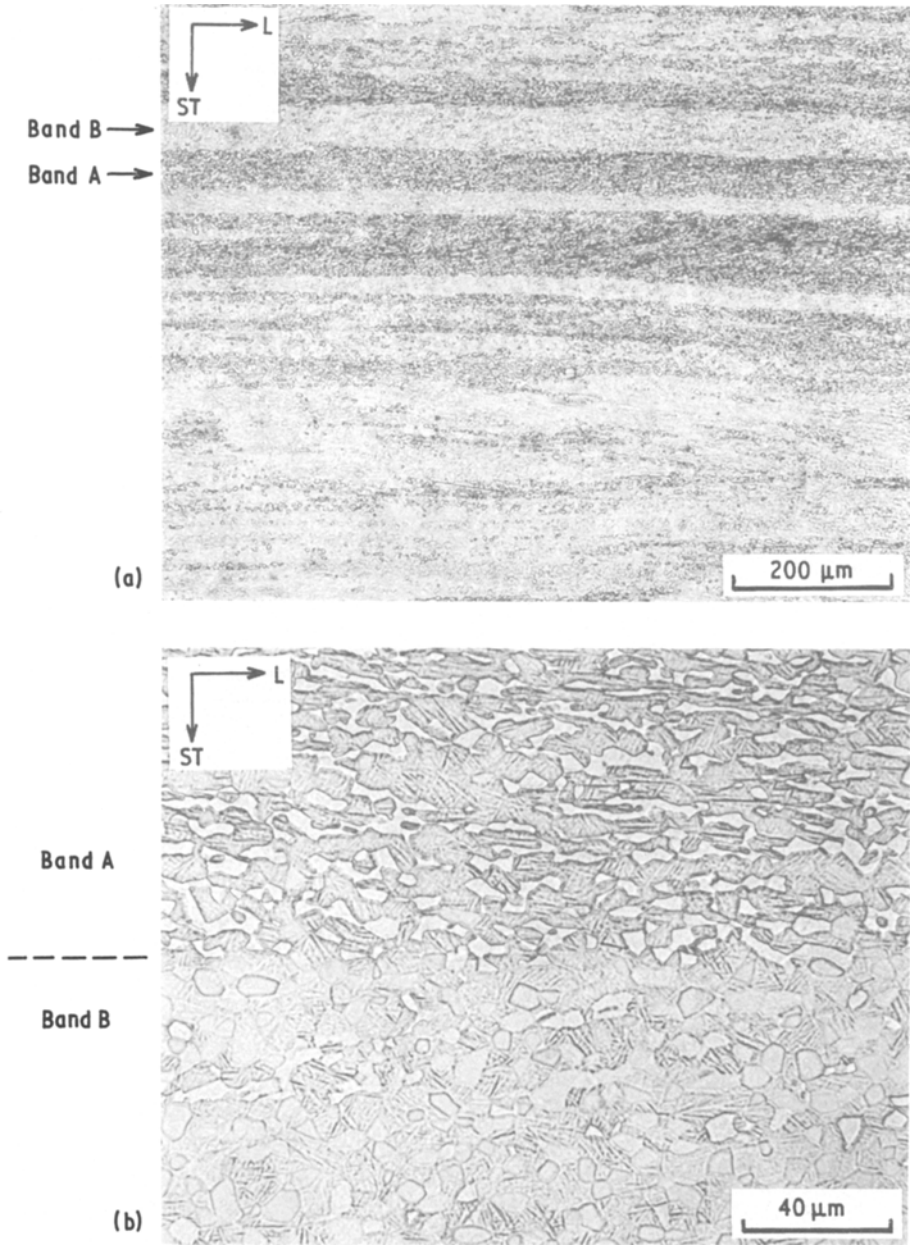

Figure 3 Initial microstructure after 0.5 h at 928° C, cold water quenched.

are plotted against strain in Figs. 5 and 6. Under superplastic conditions at 928° C (Fig. 5) the ratios were greater than unity, increased with strain and were insensitive to strain rate in the range 4.2×10^{-4} to $1.05 \times 10^{-3}\,\text{sec}^{-1}$. The intensity of the edge texture was reduced after about 300% longitudinal superplastic strain (Fig. 2) but the texture type was unchanged.

Under non-superplastic conditions at $1.05 \times 10^{-2}\,\text{sec}^{-1}$ (Fig. 6) the deformation was isotropic ($\text{d}P/\text{d}N \sim 1$) up to strains of 1.2 and there was less change in the texture (Fig. 2). With increasing strain rate at 900° C the gradient of the $\text{d}P/\text{d}N$ v strain curves decreased and $\text{d}P/\text{d}N$ ratios less than unity were obtained (Fig. 6).

The decrease in the $\text{d}P/\text{d}N$ ratio reflected a change in the deformation behaviour from that controlled by grain-boundary sliding at low strain rates (when $\text{d}P/\text{d}N > 1$) to that controlled by slip at higher strain rates (when $\text{d}P/\text{d}N < 1$). The triaxially stressed necked regions of the gauge length (dotted curves in Fig. 6) appeared to deform with less anisotropy.*

The change in the $\text{d}P/\text{d}N$ ratio at 900° C from < 1 to > 1 (Fig. 6) coincided with a change from uniform to non-uniform diametral strain which led to multiple necks as shown in Fig. 7; non-uniform diametral strain only occurred under superplastic conditions. The development of multiple necks is shown in Fig. 8 for a test piece superplastically deformed initially to 31% elongation and then to 118% elongation at 900° C and $\dot{\varepsilon}_1 = 4.2 \times 10^{-4}\,\text{sec}^{-1}$. The multiple necks could be related to differences in the grain-boundary sliding resistance in Bands A and B microstructure (Fig. 3). Cross-sections containing a high proportion of Band A microstructure deformed less and became more pronounced with increasing strain compared with cross-sections containing predominantly Band B

*It should be noted that an elliptical shaped cross-section with a given $\text{d}P/\text{d}N$ value produced by anisotropic deformation remains relatively unchanged if the deformation subsequently becomes isotropic [5]; the dotted lines in Figs. 5 and 10 therefore indicate a tendency towards isotropic deformation in the necked regions.

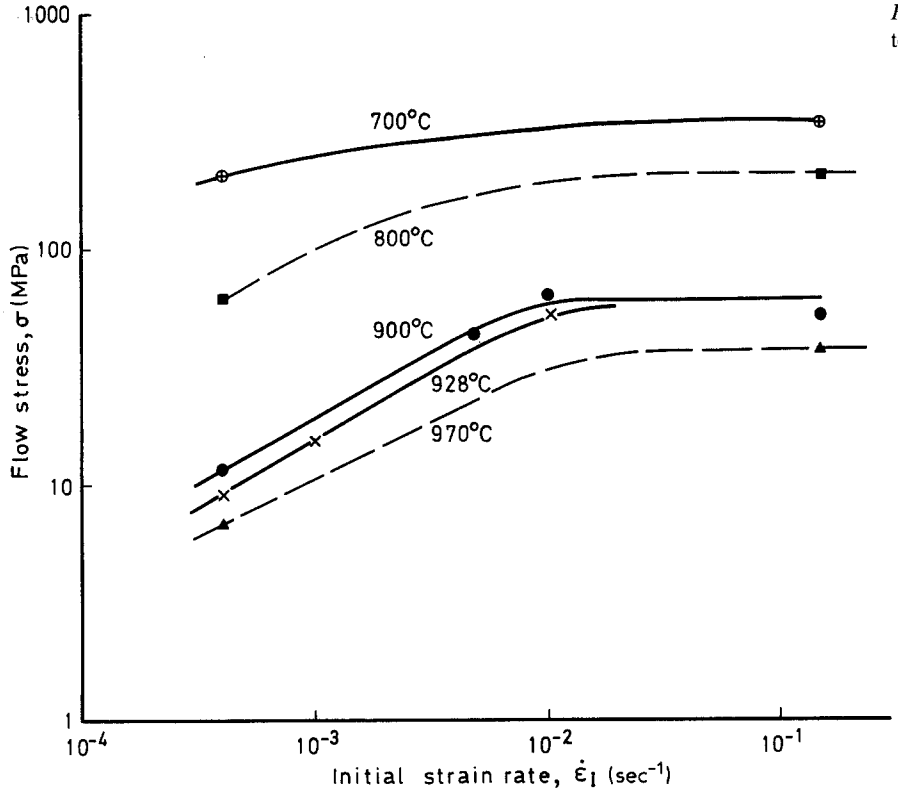

Figure 4 Effect of strain rate and test temperature on the flow stress.

microstructure. This is shown in Fig. 9, where the dP/dN ratio for a given superplastic strain was less for Band A than for Band B microstructure. Multiple necking was less pronounced in the 13 mm than in the 4 mm diameter test pieces; this was attributed to the overlapping of Bands A and B within the thicker section.

Multiple necking increased the scatter in dP/dN values for superplastically deformed test pieces as shown in Fig. 5 for 928° C and Fig. 9 for 900° C tests. For clarity the curve for 900° C in Figs. 6 and 10 is the mean of the data in Fig. 9.

3.2. Effect of test temperature

Curves of dP/dN ratio against strain were obtained at low ($\dot{\varepsilon}_I = 4.2 \times 10^{-4} sec^{-1}$) and high ($\dot{\varepsilon}_I = 1.05 \times 10^{-1} sec^{-1}$) strain rates in the temperature range 20 to 970° C. At the lower strain rate (Fig. 10a) the gradients of the curves increased with increasing temperature up to 900° C and then decreased in the range 900 to 970° C but at the higher strain rate (Fig. 10b) the gradients increased with increasing temperature throughout the temperature range. With the exception of the curves for 970° C the gradients were less at the higher strain rate.

Deformation appeared to be isotropic at 800° C at the lower strain rate (Fig. 10a) although significant α-phase was present (Fig. 11). Increasing the strain rate at this temperature changed the dP/dN ratio from unity to less than unity (Fig. 10b) and also led to a change in the diametral strain from non-uniform to uniform as shown in Fig. 12. This isotropic

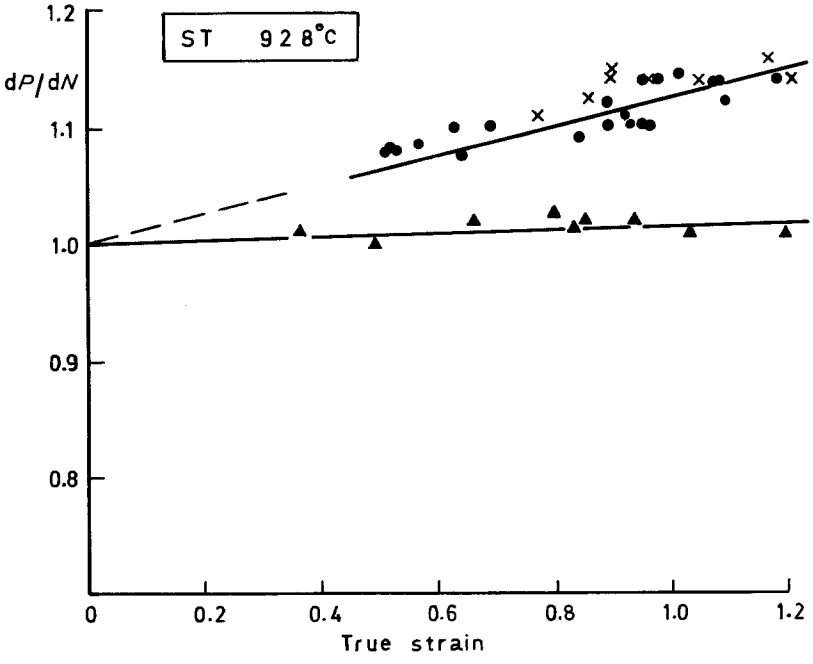

Figure 5 dP/dN ratio plotted against strain for 13 mm diameter test pieces. Superplastic; ● $\dot{\varepsilon}_I = 4.2 \times 10^{-4} sec^{-1}$, × $\dot{\varepsilon}_I = 1.05 \times 10^{-3} sec$ ▲ Non- superplastic, $\dot{\varepsilon}_I = 1.05 \times 10^{-2} sec^{-1}$.

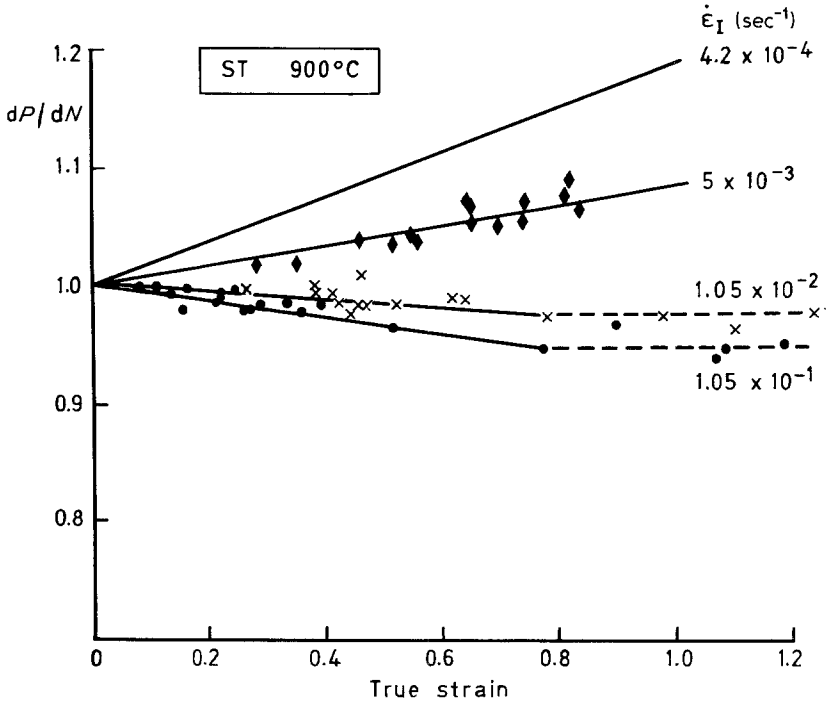

Figure 6 dP/dN ratio plotted against strain for 4 mm diameter test pieces.

deformation at 928 and 800° C occurred at the transition from slip-controlled to grain-boundary controlled deformation.

Under slip-controlled deformation (dP/dN < 1) the observed increase in dP/dN ratio with increasing temperature can be explained by the decrease in the α-phase volume fraction and the increase in $\langle c + a \rangle$ slip, which would tend to decrease the effect of α-phase texture.

When the deformation was controlled by grain-boundary sliding (dP/dN > 1) with the contiguous α-phase responsible for the anisotropy, the dP/dN ratio was expected to decrease with increasing temperature and to become unity near the β-transus. Although the dP/dN ratio was found to decrease in the temperature range 900 to 970° C (Fig. 10a), at 970° C when the α-phase volume fraction was only 13% (Fig. 11) the dP/dN values were the same at both high and low strain rates and were greater than unity (Figs. 10a and b). The 970° C test pieces always exhibited some non-uniform diametral strain (Fig. 13). Microstructure examination revealed that residual α-phase tended to concentrate in stringers. These isolated stringers were believed to be responsible for the observed anisotropy at 970° C.

The effect of axial strain and test temperature on the dP/dN ratio is shown in Fig. 14 for the lower strain rate ($\dot{\epsilon}_I = 4.2 \times 10^{-4}$ sec^{-1}). The dP/dN ratio increased with strain under grain-boundary sliding

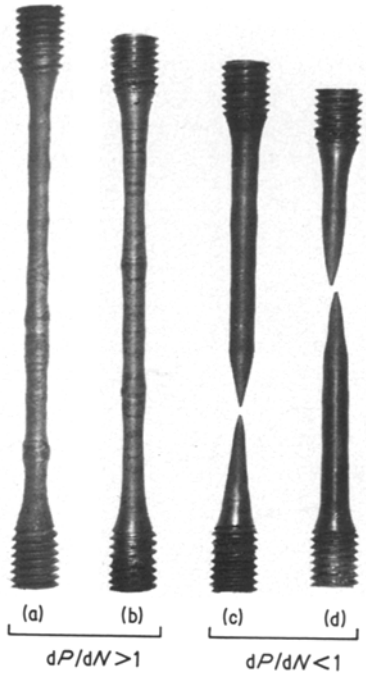

Figure 7 Effect of strain rate at 900° C on deformation. (a) 4.2 × 10^{-4} sec^{-1}, (b) 5 × 10^{-3} sec^{-1}, (c) 10^{-2} sec^{-1}, (d) 10^{-1} sec^{-1}. shown same size.

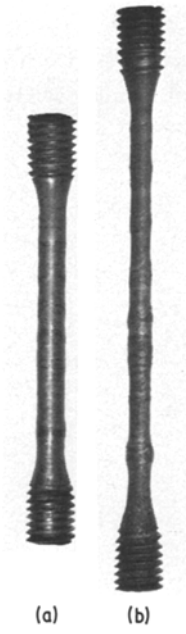

Figure 8 Effect of strain at 900° C and $\dot{\epsilon}_I = 4.2 \times 10^{-4}$ sec^{-1} on deformation. (a) 31%, (b) 118%. Shown same size.

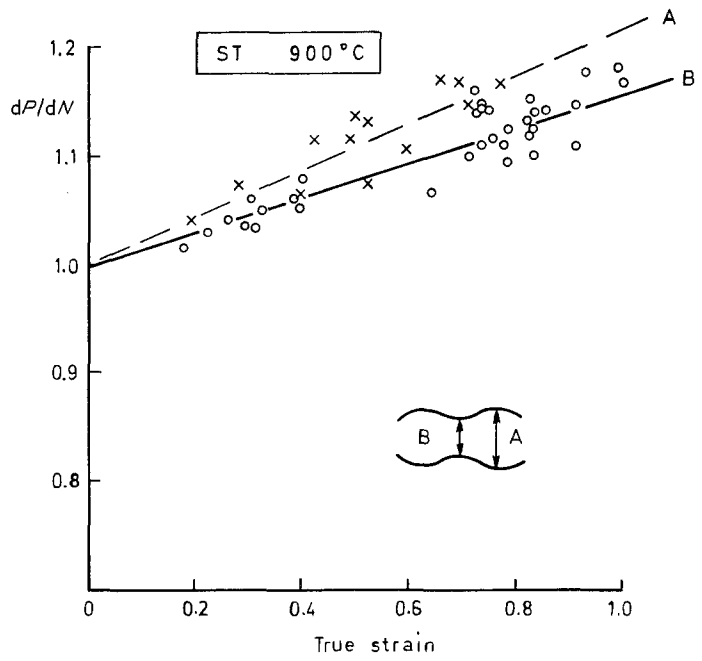

Figure 9 dP/dN ratio plotted against strain at 900° C for test piece exhibiting non-uniform diametral strain.

conditions and was a maximum at about 900° C corresponding to about 60% α-phase volume fraction.

4. Discussion

The measurement of dP/dN ratio provides a unique method for detecting the transition from grain-boundary sliding to slip controlled deformation in Ti–6Al–4V alloys. The technique is particularly suitable for highly textured two-phase alloys with an aligned microstructure. The results suggest that for Ti–6Al–4V alloy isotropic deformation under both grain-boundary sliding and slip conditions would be obtained for sheet with ⟨0002⟩ poles normal to the sheet plane and equiaxed and uniformly dispersed α- and β-phases. Since non-uniform strain was more pronounced in 4 mm than 13 mm diameter test pieces, thin sheet may be more sensitive to any aligned α-phase.

A change in the dP/dN ratio from greater than to less than unity coincided with a change from non-uniform to uniform diametral strain along the test piece gauge length. When dP/dN > 1 the *anisotropy* in the diametral strain was characteristic of that obtained under superplastic conditions when an aligned microstructure rather than a random microstructure was deformed by grain-boundary sliding. Both the non-uniform strain and the anistropy were attributed to a greater resistance to grain-boundary sliding in the α/α grain boundaries in the contiguous α-phase Band A compared to the ease of sliding in α/β and β/β boundaries in the non-aligned Band B in Fig. 3.

When dP/dN < 1 the anisotropy obtained was characteristic of that obtained at room temperature when deformation was controlled by slip and dependent on the α-phase texture [8]. The effect of strain rate and test temperature on dP/dN ratios is summarized in Fig. 15 for a strain of 0.6. Although the influence of texture decreases as dP/dN approaches unity, at strain rates $\geqslant 10^{-2}\,\mathrm{sec}^{-1}$ texture controlled the anisotropy even at 900° C when the critical resolved shear stress for slip on ⟨a⟩ and ⟨c + a⟩ systems might be

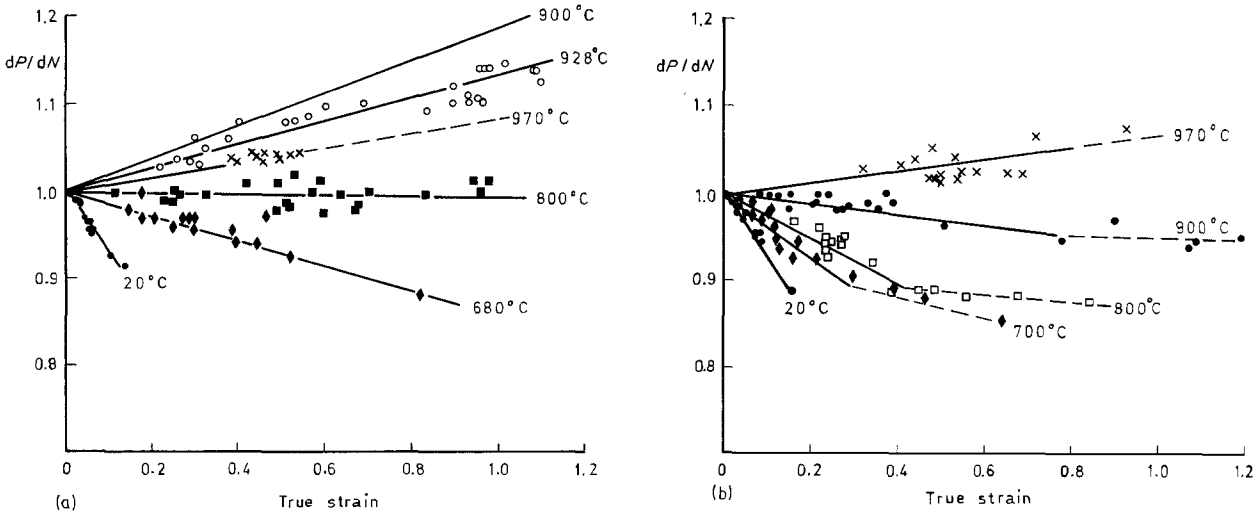

Figure 10 Effect of test temperature on dP/dN against strain curves: (a) at $\dot{\varepsilon}_1 = 4.2 \times 10^{-4}\,\mathrm{sec}^{-1}$, (b) at $\dot{\varepsilon}_1 = 1.05 \times 10^{-1}\,\mathrm{sec}^{-1}$.

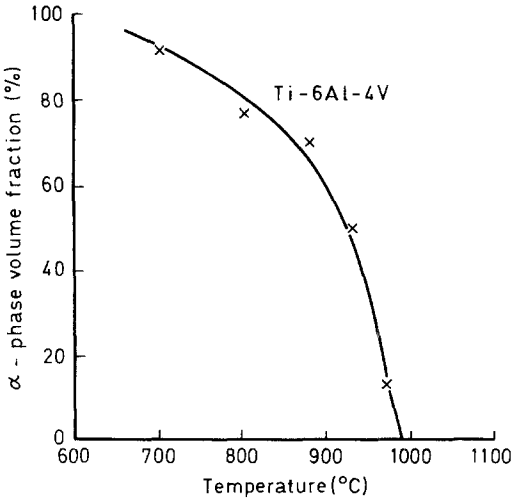

Figure 11 Effect of temperature on α-phase volume fraction in textured Ti–6Al–4V bar.

expected to be similar [9, 10]. Texture effects under these conditions were presumably caused by different strain rate sensitivity of the flow stress on the operative slip systems.

In Ti–6Al–4V at 850° C, texture was reported [11] to become random after grain-boundary sliding at very low strain rates (Stage I of the $\ln\sigma$ against $\ln\dot{\varepsilon}$ curve [1, 11]) but when dislocation processes dominated at high strain rates (Stage III of the curve) texture was retained. These observations agree with the present results since intermediate strain rates (10^{-4} to $10^{-3}\,sec^{-1}$, equivalent to Stage II) and after superplastic strains of ~300% grain-boundary sliding, reduced the texture intensity (Fig. 2). However there is evidence for a much greater change in the β-phase texture in Ti–6Al–4V [12]. The texture results suggest that during superplastic deformation of Ti–6Al–4V the α-phase behaves as relatively undeformable islands surrounded by deforming β-phase [7].

Near the deformation mode transition point ($dP/dN = 1$) the dP/dN ratio was sensitive to test

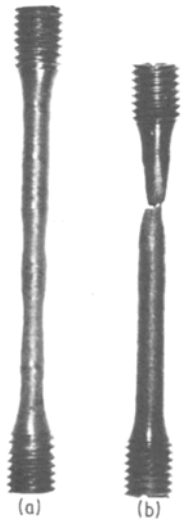

Figure 12 Effect of strain rate at 800° C on deformation. (a) $4.2 \times 10^{-4}\,sec^{-1}$, $dP/dN \sim 1$; (b) $10^{-1}\,sec^{-1}$, $dP/dN < 1$. Shown same size.

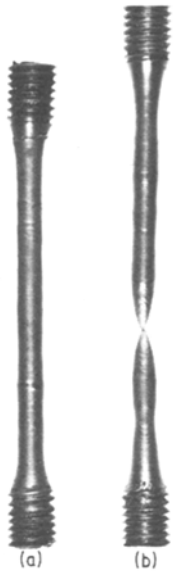

Figure 13 Effect of strain rate at 970° C on deformation. (a) $4.2 \times 10^{-4}\,sec^{-1}$, $dP/dN > 1$; (b) $10^{-1}\,sec^{-1}$, $dP/dN < 1$. Shown same size.

conditions (Fig. 13). This sensitivity may explain why superplasticity has been reported by some workers to be texture-dependent [10, 13, 14] and by others [5, 15] to be texture-independent. It follows that a reduction in forming temperature to reduced manufacturing costs [16] may lead not only to higher forming pressures but to texture-dependent anisotropy, even though high strains may be achieved.

The results obtained at 970° C were unexpected since the largely β-phase microstructure was expected to deform isotropically. However, the observed anisotropy appeared to be related to residual aligned α-phase which was probably associated with slight segregation of alloying elements. This segregation and the reduced strain rate sensitivity with increasing α-phase could be responsible for the large multiple necks at high strain rates of $10^{-1}\,sec^{-1}$ (Fig. 13b).

5. Conclusions

1. Diametral strain anisotropy measured by dP/dN, where dP and dN are the strains in two orthogonal directions, can be used to monitor the change in the controlling deformation mode in Ti–6Al–4V.

2. With increasing strain rate or decreasing test temperature a transition occurred from grain-boundary sliding ($dP/dN > 1$) controlled deformation to slip-controlled ($dP/dN < 1$) deformation.

3. The transition in deformation mode coincided with a change from non-uniform to uniform diametral strain along the test piece gauge length; the non-uniform strain was caused by the resistance to grain-boundary sliding between contiguous α-phase.

4. At 970° C when only 13% α-phase was present, anisotropy was apparent and was independent of strain rate; this was attributed to the concentration of aligned α-phase into bands.

5. A change from texture-dependent to texture-independent formation can occur with slight changes in the superplastic forming conditions near the deformation transition point.

Figure 14 Effect of strain (ε) on dP/dN plotted against test temperature.

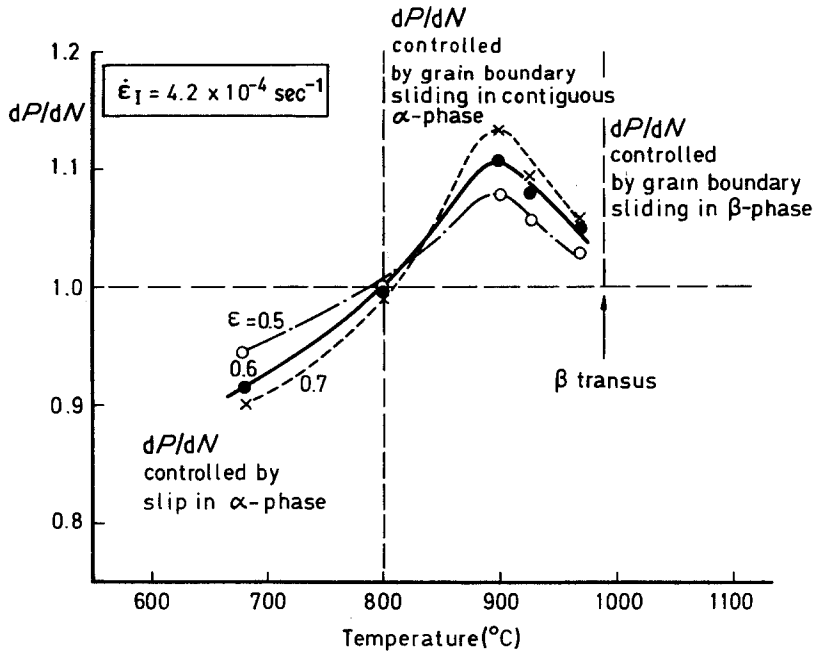

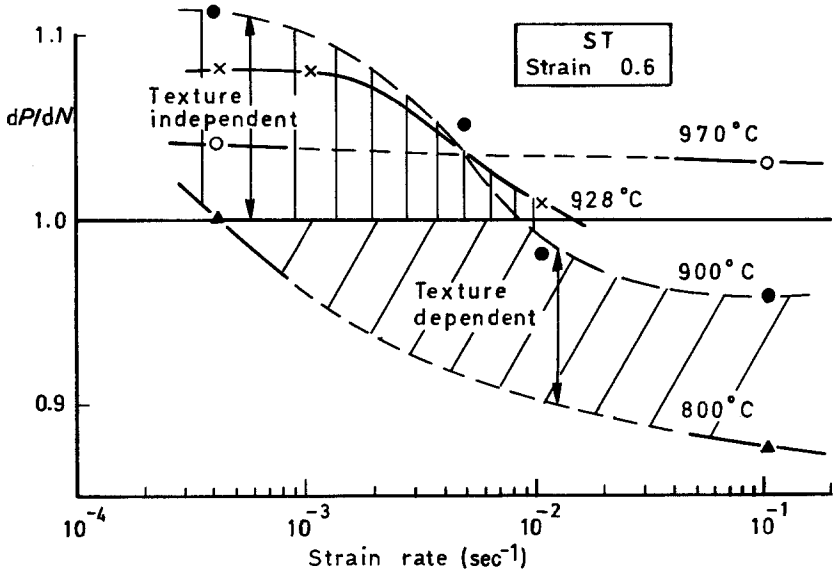

Figure 15 Effect of strain rate and temperature on the texture dependence.

Acknowledgement

This paper is published by permission of the Royal Aircraft Establishment, Crown Copyright © Controller, Her Majesty's Stationary Office, London, 1985.

References

1. K. A. PADMANABHAN and G. J. DAVIES, "Superplasticity Materials Research and Engineering", Vol. 2 (Springer Verlag, Berlin, 1980).
2. S. M. L. SASTRY, R. J. LEDERICH, T. L. MACKAY and W. R. KERR, *J. Metals* **35** (1983) 48.
3. A. E. GRECKINLI, *Metal Sci.* **17** (1983) 12.
4. M. E. ROSENBLUM, P. R. SMITH and F. H. FROES, *Titanium '80* **2** (1980) 1015.
5. D. S. McDARMAID, A. W. BOWEN and P. G. PARTRIDGE, *J. Mater. Sci.* **19** (1984) 2378.
6. *Idem, ibid.* **20** (1985) 1976.
7. P. G. PARTRIDGE, D. S. McDARMAID and A. W. BOWEN, *Acta Metall.* **33** (1985) 571.
8. P. J. E. FORSYTH and C. A. STUBBINGTON, *Metals Tech.* April (1975) 158.
9. N. E. PATON, J. C. WILLIAMS and G. P. RAUSCHER, *Titanium Sci. Technol.* **2** (1973) 1049.
10. M. PETERS, P. J. WINKLER and W. BUNK, Proceedings 5th International Conference on Titanium Munich 1984, (Deutsche Gesellschaft F. Metallkde, 1985) p. 681
11. S. M. L. SASTRY, P. S. PAO and K. K. SANKARAN, *Titanium '80* **2** (1980) 873.
12. D. S. McDARMAID, A. W. BOWEN and P. G. PARTRIDGE, RAE Tech Report 83066 (1983).
13. O. A. KAIBYSHEV and I. V. KASACHKOV, *J. Mater. Sci.* **16** (1981) 2501.
14. O. A. KAIBYSHEV, I. V. KASACHKOV and I. V. ALEXANDROV, *Acta Metall.* **32** (1984) 585.
15. N. E. PATON and C. H. HAMILTON, *Metall. Trans.* **10A** (1979) 241.
16. J. A. WERT and N. E. PATON, *ibid.* **14A** (1983) 2535.
17. C. H. HAMILTON, A. K. GHOSH and M. M. MAHONEY, "Advanced Processing Methods for Titanium", edited by D. F. Hassom and C. H. Hamilton (Metallurgical Society of AIME, 1982) p. 129.

Received 7 March
and accepted 20 March 1985